Laser cooling with adiabatic transfer on a Raman transition

Laser cooling with adiabatic transfer on a Raman transition

G P Greve[1], B Wu[1], and J K Thompson[1]

JILA, NIST, and Department of Physics, University of Colorado, 440 UCB, Boulder, CO 80309, USA

E-mail: graham.greve@colorado.edu

Abstract. Sawtooth Wave Adiabatic Passage (SWAP) laser cooling was recently demonstrated using a narrow-linewidth single-photon optical transition in atomic strontium and may prove useful for cooling other atoms and molecules. However, many atoms and molecules lack the appropriate narrow optical transition. Here we use such an atom, ^{87}Rb, to demonstrate that two-photon Raman transitions with arbitrarily-tunable linewidths can be used to achieve 1D SWAP cooling without significantly populating the intermediate excited state. Unlike SWAP cooling on a narrow transition, Raman SWAP cooling allows for a final 1D temperature well below the Doppler cooling limit (here, 25 times lower); and the effective excited state decay rate can be modified in time, presenting another degree of freedom during the cooling process. We also develop a generic model for Raman Landau-Zener transitions in the presence of small residual free-space scattering for future applications of SWAP cooling in other atoms or molecules.

Keywords: laser cooling, rubidium, Landau-Zener transitions, spontaneous emission, molecule cooling

1. Introduction to SWAP cooling

Advances in laser cooling techniques have opened new scientific vistas for neutral atoms, ions, and mechanical resonators [1, 2, 3]. Doppler cooling techniques have been widely applied to produce atoms at mK to sub-μK temperatures and high phase-space density [4, 5, 6, 7, 8, 9, 10, 11, 12]. However, standard Doppler cooling is limited in both final temperature and maximum force by the linewidth Γ and wavelength $\lambda \equiv 2\pi/k$ of the available optical transitions – properties that are provided by nature and not under control of the experimentalist. Understanding methods and limitations for removing entropy from a system is of fundamental interest and continues to be widely explored [13, 14, 15, 16, 17, 18, 19].

Further, the current challenge of extending Doppler cooling to molecules [20, 21, 22] is difficult. After each photon absorption event, a molecule needs to return to the initial state via spontaneous emission for Doppler cooling to work, but it may be lost instead due to the abundance of accessible vibrational and rotational degrees of freedom [20, 21]. This challenge has motivated the development of alternative techniques that rely on reducing the role of spontaneous emission relative to Doppler cooling, including Sisyphus cooling of molecules [18, 23], bichromatic force slowing and cooling [16, 24], and interferometric cooling [19].

Recently, a new mechanism called Sawtooth Wave Adiabatic Passage (SWAP) cooling was observed using a narrow-linewidth optical transition in ^{88}Sr atoms [25], and a related deflection force was previously reported in He atoms [26]. The SWAP technique has now been used for slowing Dy [27] and for creating faster, denser Sr magneto-optical traps [28, 29]. The forces that give rise to SWAP cooling rely on adiabatic transitions back and forth between a ground state $|a\rangle$ and a long-lived optically excited state $|b\rangle$ with lifetime $\tau = 1/\Gamma$. This allows for many photon-recoils worth of momentum reduction before spontaneous emission occurs, but so far, SWAP cooling has been limited to single-photon transitions.

In this paper, we present proof-of-principle experiments in ^{87}Rb to demonstrate that the SWAP cooling mechanism does not require a closed, single-photon transition. Rather, it is amenable to atoms and molecules with at least two long-lived ground states. The core idea is to dress these ground states (here labeled $|a\rangle$ and $|b\rangle$) using externally applied lasers tuned off-resonance from an intermediate optically excited state $|i\rangle$. This permits us to engineer effective optically excited states with tunable lifetimes or, equivalently, linewidths instead of relying on the properties of the optical transitions $|a, b\rangle \leftrightarrow |i\rangle$ (figure. 1(a)). In this manner, the limitations placed by spontaneous emission can be bypassed: the Doppler temperature associated with the intermediate state no longer applies, and there is a decreased loss rate to unwanted states. Unlike the previous report of SWAP cooling with ^{88}Sr, we achieve an equilibrium temperature in 1D that is 25 times lower than the usual $T_D \approx \frac{\hbar\Gamma}{2k_B} = 146$ μK cooling limit for standard Doppler cooling in ^{87}Rb.

In SWAP cooling using a single-photon transition, the magnetic field gradients,

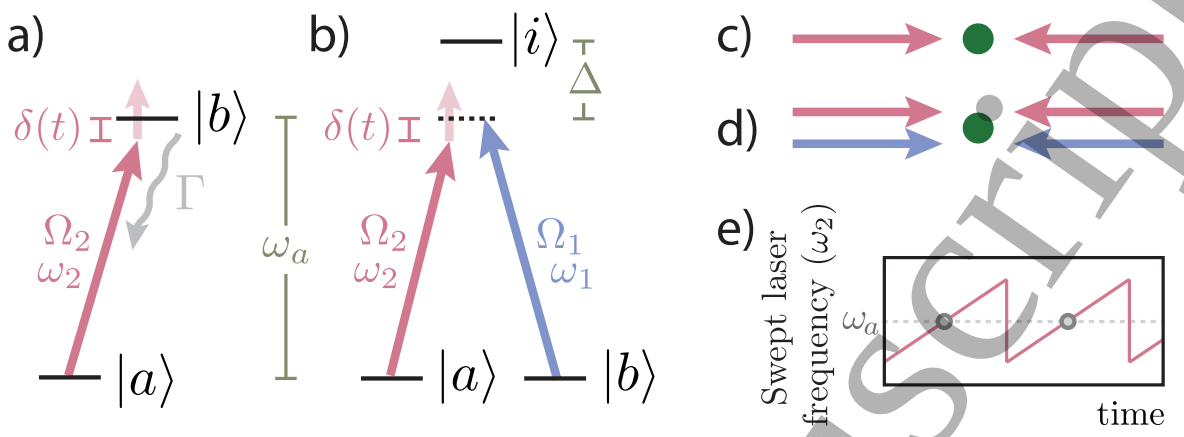

Figure 1. SWAP cooling level diagram for **(a)** a single-photon narrow-linewidth transition and **(b)** a two-photon Raman transition. In the Raman scheme, the large detuning Δ from the intermediate state ensures the effective lifetime of the excited state $|b\rangle$ is effectively infinite except when it is useful to induce decay back to $|a\rangle$ following each sweep. **(c)** In the single-photon case, the ω_2 laser (red) is counter-propagating and incident upon an atom (green). **(d)** The two-photon case is identical except a second ω_1 laser (blue) serves to dress the $|b\rangle$ state. **(e)** The frequency of ω_2 is sawtooth-swept through the atomic transition frequency.

laser directions, and polarizations are essentially identical to those of standard Doppler cooling except that the pair of counter-propagating laser beams are ramped in frequency in a sawtooth pattern from below to above the transition frequency ω_a (figure. 1(c and e)). The relative Doppler shift of the two laser beams causes the beam counter-propagating to the atom's motion to pass through resonance before the co-propagating beam. As a result, the counter-propagating beam drives an adiabatic transition from $|a\rangle$ to $|b\rangle$ along with a momentum kick due to photon absorption that opposes the atomic motion. The co-propagating beam then drives an adiabatic transition back from $|b\rangle$ to $|a\rangle$ along with a momentum kick due to stimulated emission that, again, slows the atom. In net, each sweep ideally removes $2\hbar k$ of momentum, reducing the atom's speed regardless of the direction it is moving.

In SWAP cooling using a two-photon transition, an additional, fixed laser frequency dresses the ground state $|b\rangle$ (figure. 1(d)). The laser dressing the ground state $|a\rangle$ is swept in an asymmetric sawtooth pattern through a two-photon resonance, driving adiabatic Raman transitions between the states $|a\rangle$ and $|b\rangle$. Details of magnetic fields and polarizations will be addressed below. At the end of the sweep, optical pumping is briefly applied to transfer atoms erroneously remaining in $|b\rangle$ back to $|a\rangle$. In comparison to the work in strontium [25], this is equivalent to being able to set $\Gamma \approx 0$ during the frequency sweep, but then setting Γ up to the lifetime of the intermediate state for a very brief period of time in between sweeps, potentially offering a different degree of freedom for optimizing cooling.

2. Laser cooling rubidium with adiabatic transfers

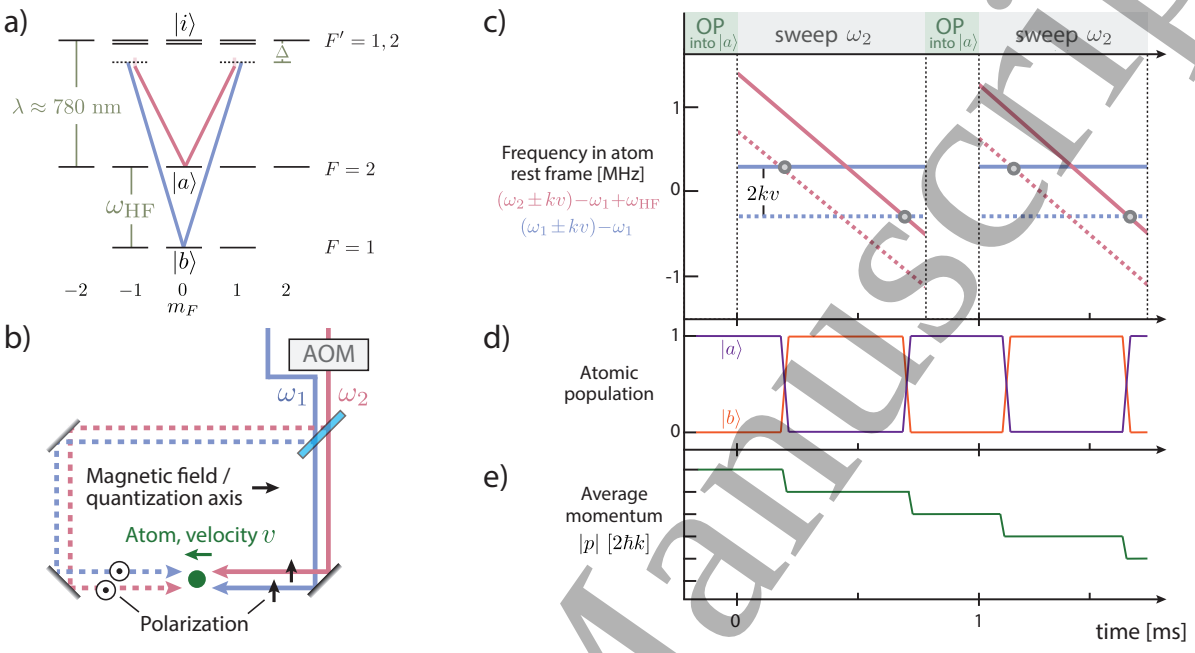

Figure 2. **(a)** ^{87}Rb level diagram. Two-photon transitions between $|a\rangle$ and $|b\rangle$ are induced by ω_1 (blue) and ω_2 (red). **(b)** Experimental layout. A moving atom (green) interacts with two pairs of counter-propagating laser beams (blue, red) with ω_2 varied in a saw-tooth manner. Orthogonal linear polarizations are indicated by solid and dashed lines. **(c)** The four unique laser frequencies observed in the rest frame of the atom after including the Doppler shifts that separate counter-propagating lasers in frequency by $2kv$. Offsets have been subtracted so that points marked with circles correspond to allowed two-photon resonances which involve pairs (solid and dashed lines) of orthogonally-polarized, counter-propagating laser beams. **(d)** Two-photon Landau-Zener transitions transfer an atom from $|a\rangle$ to $|b\rangle$ and back to $|a\rangle$ each sweep. **(e)** The counter-propagating lasers and sweep direction ideally remove $4\hbar k$ momentum per cooling sweep.

Figure 2 shows the experimental setup for demonstrating 1D Raman SWAP cooling in ^{87}Rb. The quantization axis is established by a uniform magnetic field applied along the propagation axis of the cooling beams. The two ground states are the hyperfine Zeeman states $|a\rangle \equiv |F = 2, m_F = 0\rangle$ and $|b\rangle \equiv |F = 1, m_F = 0\rangle$. These states are coupled by lasers at frequencies ω_1 and ω_2, both far-detuned from the intermediate state $|i\rangle$ by an amount $\Delta \approx 2\pi \times 2$ GHz. The allowed two-photon transitions involve absorption and stimulated emission of pairs of orthogonal linearly polarized photons differing in frequency by the ground state hyperfine splitting of $\omega_{\rm HF} = 6.834$ GHz. The cooling beams incident from the left are vertically polarized and the beams incident from the right are horizontally polarized. Dipole selection rules disallow two-photon transitions with pairs of photons of the same linear polarization, *i.e.*, the only allowed two-photon Raman transitions are those that also impart a net photon recoil momentum $2\hbar k$ as the internal state changes.

Both beam directions have two distinct frequency components ω_1 and ω_2 (figure 2(b)) created by combining the output of two phase-locked lasers. We choose to hold the frequency ω_1 fixed while the frequency component ω_2 is swept linearly in time downward in frequency through the two-photon atomic resonance at $\omega_1 - \omega_2 \approx \omega_{\mathrm{HF}}$.

Accounting for Doppler shifts of the laser frequencies as seen by an atom moving at speed v, there are two two-photon resonances that occur when $\delta(t) \equiv \omega_1 - \omega_2 - \omega_{\mathrm{HF}} = \pm 2kv$ (figure 2(c)). Ideal adiabatic passage through each resonance imparts a net momentum kick of $2\hbar k$ per transition, *i.e.* $4\hbar k$ per sweep. The direction of the frequency sweep is chosen such that the time ordering of the passage through the two resonance frequencies leads to a reduction of the atom's speed in the laboratory frame.

As the atom approaches zero speed and the Doppler shift is of the same order as Ω_{ab}, there is no longer a preferred time-ordering for the adiabatic transfers detailed above, and the cooling mechanism fails. Here, $\Omega_{\mathrm{ab}} \approx \frac{\Omega_1 \Omega_2}{2\Delta}$ is the two-photon Rabi frequency and $\Omega_1 \approx \Omega_2$ are the single-photon Rabi frequencies of each frequency component. With the inevitable failure of a transfer, either due to broken time-ordering or imperfect adiabatic transfer, an atom can have considerable probability to be in $|b\rangle$ following a sweep so that the next iteration results in heating. We apply π-polarized optical pumping light from a direction orthogonal to the cooling beams to return any atoms remaining in $|b\rangle$ to $|a\rangle$ before the next frequency sweep. The optical pumping was applied here for 100 μs, though this is much longer than required to achieve efficient optical pumping.

In our experiment, around 10^7 atoms are loaded into a magneto-optical trap (MOT) and pre-cooled to about 42 μK with polarization gradient cooling (PGC) to narrow the initial velocity distribution and lessen the requirements on the sweep's effective capture range. The atoms are optically pumped into $|a\rangle$. Frequency sweeps are then applied with typical sweep times of 1 ms and sweep range 1 MHz as shown in figure 2(c). The ideal internal state populations and change in momentum are shown in figure 2(d and e). This sequence of optical pumping and sweeping is repeated several times. The final 1D temperature of the atoms is measured by velocimetry. All atoms are optically pumped back to $|a\rangle$ and then velocity-selective Raman transitions drive atoms within a small velocity range into $|b\rangle$ [30]. The population in $|b\rangle$ is determined using fluorescence and the resulting Voigt profiles are fit to extract the temperature (figure 3(a)).

We observe cooling from an initial temperature of 42(3) μK to 10 μK after the application of 9 sweeps with fixed two-photon Rabi frequency $\Omega_{\mathrm{ab}} = 2\pi \times 22$ kHz and sweep range of $\Delta_{\mathrm{swp}} \equiv 2\pi \times 0.8\,\mathrm{MHz}$ (purple points in figure 3(b)). The sweep range is chosen to allow over 95% of the atoms to pass through two-photon resonance during the sweep when accounting for the Doppler shifts of the initial velocity distribution of the atoms.

The temperature can be reduced by progressively decreasing the two-photon Rabi frequency and the sweep range, as is done for the green points in figure 3(b). After the first three sweeps (purple points), the Rabi frequency is reduced to $\sqrt{0.5} \times \Omega_{\mathrm{ab}}$ and the the sweep range is reduced to $0.5 \times \Delta_{\mathrm{swp}}$ such that the Landau-Zener adiabaticity parameter ξ (discussed below) is unchanged. The sweep range can be reduced because the velocity

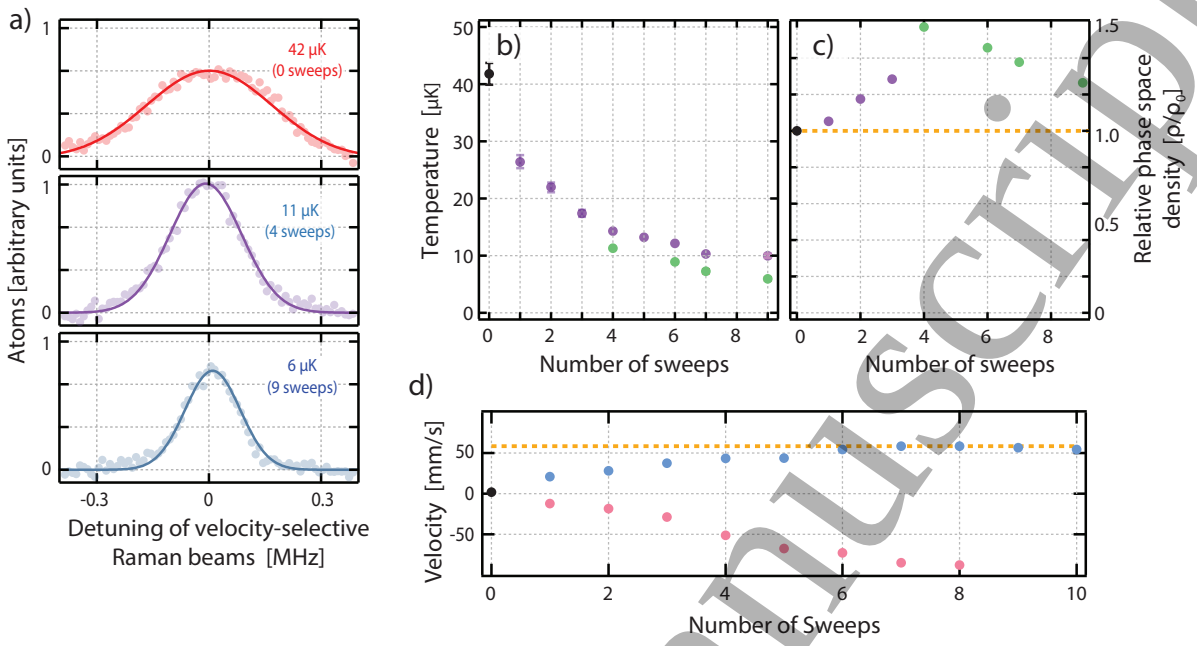

Figure 3. **(a)** The reduction in temperature is determined by measuring the initial velocity distribution (red) and the distribution after four and nine sweeps (purple and blue). The velocity distributions shown here are determined by driving Raman transitions that are only resonant for atoms in a narrow velocity-class whose center is set by the detuning of the Raman beams. **(b)** The atomic ensemble is cooled as low as 5.9 μK in one dimension over the course of several sweeps. For the purple points, all sweeps used a two-photon Rabi frequency $\Omega_{\rm ab} \approx 2\pi \times 22$ kHz and sweep range $\Delta_{\rm swp} = 2\pi \times 0.8$ MHz. For the green points, $\Omega_{\rm ab}$ and $\Delta_{\rm swp}$ were successively reduced between sweeps as described in the text. **(c)** The relative one-dimensional phase-space density for the corresponding purple or green points in (b). The phase-space density begins to decrease after four sweeps despite the decreasing temperature because atoms begin to leave the velocimetry beams. **(d)** To cool into a moving reference frame (blue points), we apply a frequency offset $\delta_{\rm AOM} = 2\pi \times 150$ kHz in the lab reference frame between the beams from opposite directions. By sweeping ω_2 downwards, the atoms cool and equilibrate into a moving reference frame which has a velocity $v_F \equiv \delta_{\rm AOM}/2k$ (dashed orange line). If the sweep direction is reversed (pink points), the atoms accelerate in the opposite direction without being bound by $|v_F|$.

distribution was reduced by the initial sweeps. After two sweeps, the remaining sweeps are performed with two-photon Rabi frequency $\sqrt{0.4} \times \Omega_{\rm ab}$ and sweep range $0.4 \times \Delta_{\rm swp}$. After 9 total sweeps, the measured temperature reaches 5.9(3) μK.

An increase in phase-space density demonstrates a reduction of entropy and not merely a selective loss of atoms or a redistribution of the density in phase space. In figure 3(c), we see that the the relative 1D phase space density $\rho/\rho_0 = \Delta x_0 \Delta v_0/(\Delta x \Delta v)$ is increased, where Δx and Δv (Δx_0 and Δv_0) are the measured cloud size and velocity spread after (before) cooling. Given that phase space compression cannot occur without dissipation, the lack of spontaneous emission in an ideal sweep is initially alarming. But one can achieve phase space compression without actually scattering a photon – it is sufficient that the atom could have scattered a photon were it within a particular

region of phase space. When an atom's Doppler shift $kv \lesssim \Omega_{\rm ab}$ and there is significant probability of finishing a sweep in the wrong internal state, a scattered optical pumping photon signals that an atom has a velocity $kv \lesssim \Omega_{\rm ab}$. In the early cooling stages, when $kv \gg \Omega_{\rm ab}$, the atom is always moved towards lower velocity without scattering a photon, but even *not scattering* a photon acts as information to the environment that reduces the probability that the atom is in the portion of phase space with $kv < \Omega_{\rm ab}$.

The Raman adiabatic transitions we use are distinct from stimulated Raman processes in velocity-selective coherent population trapping [31] or schemes related to Raman cooling [32, 33]. In addition, the polarization scheme here is reminiscent of polarization gradient cooling [34], but here there is a large magnetic field present that breaks the degeneracy of ground states that is typically required for polarization gradient cooling to such a low temperature. Furthermore, when the sweep direction was reversed, we observed heating as expected in the SWAP model of cooling.

To further emphasize the critical role of the sweep direction in the present work, we apply a fixed relative offset frequency $\delta_{\rm AOM}$ between the counter-propagating beams such that one would expect that atoms are cooled into a moving reference frame with velocity $v_F = \delta_{\rm AOM}/2k$. If the laser frequency is swept downward as was done for the cooling experiments above, we observe that the atoms are accelerated into and equilibrate into the moving frame (blue points in figure 3(d)). The orange dashed line indicates the velocity of the predicted moving frame for the applied frequency offset $\delta_{\rm AOM} = 2\pi \times 150\,\text{kHz}$. In contrast, if we simply reverse the frequency sweep direction, we observe that the atoms are accelerated in the opposite direction despite the direction of the moving reference frame remaining unchanged (pink points of figure 3(d)). The atoms are accelerated to speeds larger than the calculated $|v_F|$ as expected.

3. Adiabatic transfer in the presence of scattering

The choice of sweep rate $\alpha \equiv \mathrm{d}\omega_2/\mathrm{d}t$ is optimized by considering two effects. First, to achieve highly efficient adiabatic transfer, the laser frequency should be swept slowly such that the ideal Landau-Zener diabatic transition probability is small, $P_d = e^{-\xi} \ll 1$ where $\xi = \frac{\pi}{2}\Omega_{\rm ab}^2/\alpha$. Second, to avoid off-resonant spontaneous scattering of light from the applied cooling laser beams, the probability to have not scattered a photon during the total sweep time is ideally close to unity, $P_{\rm sc} = e^{-R_{\rm sc}\Delta_{\rm swp}/\alpha} \approx 1$, and hence the sweep cannot be excessively slow. $R_{\rm sc}$ is the total spontaneous scattering rate from the far-from-resonance intermediate state(s).

In figure 4(a) (circles), we measure the probability to successfully transfer from $|a\rangle$ to $|b\rangle$ after a single adiabatic transfer using σ^+ polarized beams from a single direction and such that the two-photon Rabi frequency is the same as for the data in figure 3(b). This configuration allows Doppler-free, dipole-allowed transitions. The data shows that there is an optimum sweep rate α that maximizes the transfer efficiency as desired for efficient cooling. For comparison, the red dashed line is the predicted transfer efficiency $1-P_{\rm d}$ ignoring free space scattering. The measurements qualitatively match predictions

from numerically integrating optical-Bloch equations including spontaneous emission (figure 4(a) orange).

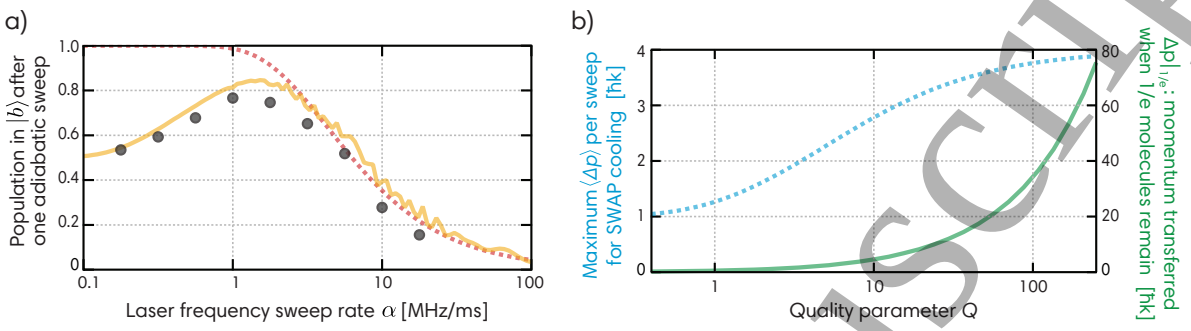

Figure 4. **(a)** Population in $|b\rangle$ after one adiabatic transfer attempt, measured using fluorescence detection (black points). Here, transitions were driven using co-propagating σ^+-polarized light with frequencies ω_1 and ω_2. ω_1 was constant and ω_2 was swept through resonance at different sweep rates $\alpha = \mathrm{d}\omega_2/\mathrm{d}t$. Transfers were performed with $(\Omega_{\mathrm{ab}}, \Gamma, \Delta, \Delta_{\mathrm{swp}}) = 2\pi \times (20\,\mathrm{kHz}, 6\,\mathrm{MHz}, 2\,\mathrm{GHz}, 0.8\,\mathrm{MHz})$. The familiar Landau-Zener prediction (red dashed) fails at low sweep rate due to off-resonant scattering from the intermediate state $|i\rangle$. A numerical simulation using the experimental parameters and including off-resonant scattering shows qualitative agreement (orange) with the data. **(b, left)** The achievable momentum transfer per SWAP cooling sweep (blue dashed) approaches the ideal $4\hbar k$ at large quality parameter $Q \equiv \frac{\pi}{2}\frac{\Omega^2}{\Gamma\Delta_{\mathrm{swp}}}$. **(b, right)** For SWAP cooling of molecules, we consider a worst-case scenario in which a molecule is lost if it undergoes a single spontaneous emission event. The predicted achievable momentum transfer when $1/e$ molecules remain (green) is shown versus the quality parameter Q.

To generalize predictions for how scattering will limit SWAP cooling, we consider the three-level system shown in figure 1(b). We will assume that the intermediate state $|i\rangle$ decays with equal rates of $\Gamma/2$ into both $|b\rangle$ and $|a\rangle$. We also assume $\Omega_1 = \Omega_2 = \Omega$, and that the large detuning limit $\Delta \gg \Gamma, \Omega$ is satisfied. The two-photon Rabi frequency is then $\Omega_{\mathrm{ab}} = \frac{\Omega^2}{2\Delta}$, and the total scattering rate is $R_{\mathrm{sc}} = \frac{\Gamma\Omega^2}{4\Delta^2}$. More details about the following treatment are provided in the Appendix.

We use this simplified system to find the optimum momentum transferred Δp during a cooling sweep after optimizing the sweep rate α. In figure 4(b, blue), we plot Δp against a dimensionless quality parameter $Q \equiv \ln P_{\mathrm{d}} / \ln P_{\mathrm{sc}} \approx \frac{\pi}{2}\frac{\Omega^2}{\Gamma\Delta_{\mathrm{swp}}}$. When $Q \gg 1$, the momentum transfer per sweep saturates to the ideal value $4\hbar k$, and the effective force is $4\hbar k/t_{\mathrm{swp}}$, where the time to complete each sweep is t_{swp}. At this optimized sweep rate, $t_{\mathrm{swp}} = \frac{8\ln(2Q)}{\pi}\frac{\Delta^2}{\Omega^4}\Delta_{\mathrm{swp}}$. In terms of experimentally controllable parameters, the quality parameter scales with laser intensity I and wavelength as $Q \propto I\lambda^3$, but does not depend on the dipole matrix element M between the states $|b\rangle$, $|a\rangle$ and the intermediate state $|i\rangle$. The sweep time scales as roughly $t_{\mathrm{swp}} \propto \frac{\Delta^2}{M^4 I^2}\Delta_{\mathrm{swp}}$.

For cooling molecules, where avoiding spontaneous emission is of chief importance, one must understand how much momentum can be removed before the molecule is lost. We take the worst case scenario, where every molecule that spontaneously emits a

photon is completely lost. In figure 4(b, green), we plot $\Delta p|_{1/e}$, the average momentum transfer when $1/e$ molecules remain, again numerically optimizing the sweep rate. For $Q \gg 1$, the numerical result is well approximated by $\Delta p|_{1/e} \approx \frac{2.1Q}{\ln(4(Q+14))}\hbar k$. By engineering systems with high quality parameter Q, one can remove many photon recoils of momentum from a molecule before it is likely to be lost. The optimized sweep time is nicely approximated by $t_{\mathrm{swp}} \approx \frac{\ln(4(14+Q))}{3.2}\frac{\Delta^2}{\Omega^4}\Delta_{\mathrm{swp}}$.

4. Conclusions

We have demonstrated that Raman transitions may be employed for SWAP cooling atoms without a single-photon narrow transition, achieving final temperatures well below the Doppler cooling limit. The technique is straightforward to implement, is amenable towards working in the presence of a large magnetic field, is robust against small changes in atomic transition frequency, and might prove useful for cooling molecules. We have also identified a quality parameter Q that provides guidance as to what experimental systems are needed for Raman SWAP cooling to work efficiently.

Future work may look towards using the technique to cool in more dimensions. In principle, 3D cooling should be possible by adding additional sets of cooling beams along $\hat{y}$ and $\hat{z}$ (where the the 1D cooling above is defined along $\hat{x}$) and cooling one dimension at a time. The direction of the magnetic field $\vec{B}$ probably cannot be changed quickly between sweeps, so the available laser polarizations become a subtle obstacle for 3D cooling. In one scheme, the magnetic field could be chosen along $\hat{x}+\hat{y}+\hat{z}$ such that some light is always projected to facilitate two-photon transitions. Then some light is also projected into π-polarization, which does not contribute to cooling but results in additional free-space scattering. In a second scheme, if ω_1 and $\vec{B}$ are kept along $\hat{x}$, while ω_2 is sent along each direction to be cooled, then sweeps along $\hat{y}$ and $\hat{z}$ maximally reduce $2\hbar k$ (rather than 4 $\hbar k$) momentum per sweep, thus leading to a slightly lower cooling rate.

It may also be interesting to explore the manipulation of ensembles via accelerations and decelerations. The initial temperature, which constrains the required sweep range Δ_{swp}, was tens of μK in this experiment, but it could potentially be orders of magnitude higher provided the available laser power still permits large Q. More complex waveforms for the laser intensity and detuning could potentially decrease the required sweep range [35], increasing the effective cooling rate.

Acknowledgments

All authors acknowledge financial support from DARPA QuASAR, ARO, NSF PFC, and NIST. This work is supported by the National Science Foundation under Grant Number 1125844.

Appendix: probabilitistic model for Raman SWAP cooling

As discussed in the main text, adiabatic transfer in the presence of scattering is optimized by a balance between the need to sweep slowly to preserve adiabaticity and the need to sweep fast enough to avoid significant scattering. Numerical simulations were used to better understand the dynamics and limitations of adiabatic passage. Here we consider a slightly simplified model: this atom (figure A1(a)) has stable ground states $|a\rangle$ and $|b\rangle$ and an optically excited state $|i\rangle$ that decays into them with equal probability at total rate Γ. The energy of these states are $\hbar\omega_\mathrm{a}$, $\hbar\omega_\mathrm{b}$, and $\hbar\omega_\mathrm{i}$. A laser at frequency $\omega_1(t)$ couples $|a\rangle \leftrightarrow |i\rangle$ with single-photon Rabi frequency Ω_1, and a laser at frequency $\omega_2(t)$ couples $|b\rangle \leftrightarrow |i\rangle$ with Rabi frequency Ω_2. The average detuning Δ of these lasers from the excited state is large compared to the two-photon detuning $\delta(t)$.

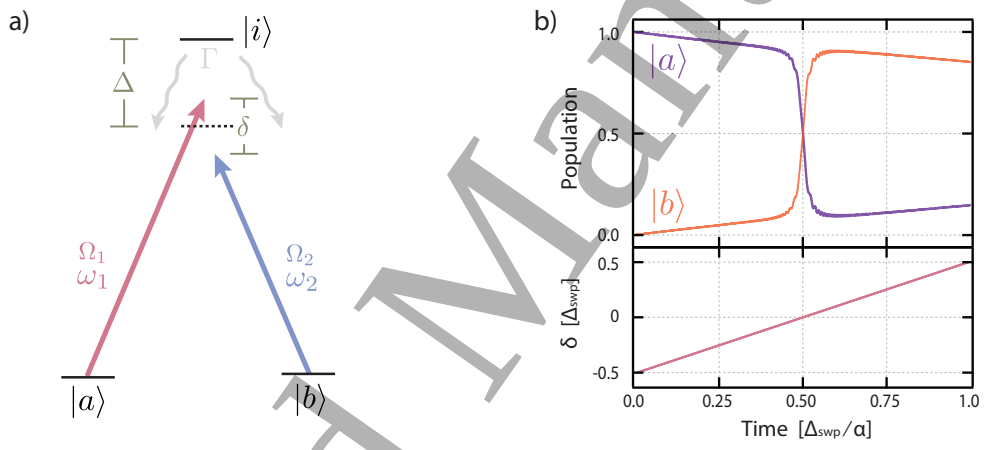

Figure A1. **(a)** Diagram for simplified three-level system. An excited state $|i\rangle$ spontaneously decays equally to $|a\rangle$ and $|b\rangle$ at total decay rate Γ. Lasers connect $|a\rangle$ and $|b\rangle$ to a state detuned from $|i\rangle$ by Δ. **(b)** Simulated time dynamics of adiabatic transfer, ignoring momentum states. In units of the scattering rate, the sweep range is $\Delta_\mathrm{swp} = \Gamma/3$, $\Delta = 300\Gamma$, $\Omega_\mathrm{ab} = \Gamma/150$. The scattering rate Γ is responsible for the coherence decay.

Adiabatic transfer from $|a\rangle$ to $|b\rangle$ adds $2\hbar k$ momentum to an atom, and transfer from $|b\rangle$ to $|a\rangle$ removes $2\hbar k$ momentum. If we assume that during a scattering process, absorption from $|a\rangle$ adds one photon's worth of momentum, and absorption from $|b\rangle$ removes one photon's worth momentum, but decay into either state causes no coherent momentum change, then to first-order, the possible change in momentum is detailed in table A1. The first-order expected change in momentum, from summing the tabulated momentum changes multiplied by the probability of that trajectory, is found to be

$$\langle \Delta p_\mathrm{AT} \rangle = \left(1 + x - 2x^{1+Q}\right) \times \hbar k$$

with $x \equiv e^{-R_\mathrm{sc}\frac{\Delta_\mathrm{swp}}{\alpha}}$, $R_\mathrm{sc} = \frac{\Gamma\Omega^2}{\Gamma^2+4\Delta^2+2\Omega^2} \approx \frac{\Gamma\Omega^2}{4\Delta^2}$, and $Q \equiv \frac{\pi}{2}\frac{\Omega^2}{\Gamma\Delta_\mathrm{swp}}$. Numerical simulations of the Bloch equations, including scattering and several momentum states, served to validate this model exceptionally well.

Row	**Before $T/2$**	**At $T/2$**	**After $T/2$**	**Probability**	Δp
1	Scatter to $\|b\rangle$	Transfer to $\|a\rangle$	Scatter	$\frac{1}{2}SAS$	$0\,\hbar k$
2	Scatter to $\|b\rangle$	Transfer to $\|a\rangle$	No scatter	$\frac{1}{2}SA(1-S)$	$-1\,\hbar k$
3	Scatter to $\|b\rangle$	No transfer	Scatter	$\frac{1}{2}S(1-A)S$	$0\,\hbar k$
4	Scatter to $\|b\rangle$	No transfer	No scatter	$\frac{1}{2}S(1-A)(1-S)$	$1\,\hbar k$
5	Scatter to $\|a\rangle$	Transfer to $\|b\rangle$	Scatter	$\frac{1}{2}SAS$	$2\,\hbar k$
6	Scatter to $\|a\rangle$	Transfer to $\|b\rangle$	No scatter	$\frac{1}{2}SA(1-S)$	$3\,\hbar k$
7	Scatter to $\|a\rangle$	No transfer	Scatter	$\frac{1}{2}S(1-A)S$	$2\,\hbar k$
8	Scatter to $\|a\rangle$	No transfer	No scatter	$\frac{1}{2}S(1-A)(1-S)$	$1\,\hbar k$
9	No scatter	Transfer to $\|b\rangle$	Scatter	$(1-S)AS$	$1\,\hbar k$
10	No scatter	Transfer to $\|b\rangle$	No scatter	$(1-S)A(1-S)$	$2\,\hbar k$
11	No scatter	No transfer	Scatter	$(1-S)(1-A)S$	$1\,\hbar k$
12	No scatter	No transfer	No scatter	$(1-S)(1-A)(1-S)$	$0\,\hbar k$

Table A1. First-order possibilities for atom state trajectories. An atom starts in $|a\rangle$ and may scatter before time $T/2$. At time $T/2$, adiabatic transfer may occur. From $T/2$ to T, the atom may scatter again. The probability to undergo adiabatic transfer is $A \equiv 1-\exp\left(-\frac{\pi}{2}\frac{\Omega_{\rm ab}^2}{\alpha}\right)$, and the probability to scatter is $S \equiv 1-\exp\left(-R_{\rm sc}\frac{\Delta_{\rm swp}}{2\alpha}\right)$ with scattering rate $R_{\rm sc} = \frac{\Gamma\Omega^2}{\Gamma^2+4\Delta^2+2\Omega^2} \approx \frac{\Gamma\Omega^2}{4\Delta^2}$.

The momentum transfer during a full SWAP cooling sweep comes from cooling during the first half of the sweep, and cooling or heating during the second half depending on if an atom successfully transferred from $|a\rangle$ to $|b\rangle$. The expected momentum transfer during a full cooling sweep is then $\langle\Delta p_{\rm SWAP}\rangle = \langle\Delta p_{\rm AT}\rangle\,(1+(P(b)-P(a)))$. The fraction of atoms cooled vs. heated in the second half of the sweep is represented by $(P(b)-P(a))$, where $P(x)$ is the probability to be in state $|x\rangle$ at the conclusion of the first half of the sweep. We find

$$\langle\Delta p_{\rm SWAP}\rangle = \langle\Delta p_{\rm AT}\rangle\left(1+x(1-2x^Q)\right). \tag{A.1}$$

To evaluate the benefits of SWAP cooling over Doppler cooling, we would like to know how much momentum could be removed before an atom (or molecule) detrimentally scatters a photon. Although we assumed equal branching ratios up until now, suppose that every scattering event causes an atom to be lost. We assume each atom scatters one photon from optical repumping if it finishes the cooling sweep in $|b\rangle$. The expected change in momentum per sweep comes entirely from the events of table A1 row 10 and 12:

$$\langle\Delta p'_{\rm AT}\rangle = (1-S)A(1-S)\times 2\hbar k = x(1-x^Q)\times 2\hbar k.$$

To be consistent, we need to normalize this to the number of atoms remaining in the system:

$$\begin{aligned}\langle\Delta p_{\rm AT}\rangle &= \frac{\langle\Delta p'_{\rm AT}\rangle}{(1-S)A(1-S)+(1-S)(1-A)(1-S)}\\ &= (1-x^Q)\times 2\hbar k\end{aligned}$$

$$\begin{aligned}\langle \Delta p_{\mathrm{SWAP}} \rangle &= \langle \Delta p_{\mathrm{AT}} \rangle \times [1 + ((1-S)A(1-S) - (1-S)(1-A)(1-S))] \\ &= \left(1 + x - x^Q - 3x^{1+Q} + 2x^{1+2Q}\right) \times 2\hbar k\end{aligned}$$

Next we choose to find the average momentum transferred per atom at a time when $1/e$ atoms remain, with the assumption that any scattering event will cause the atom to be lost. The two ways an atom does not scatter a photon (during the sweep or from optical repumping) come again from rows 10 and 12:

$$P(\text{no scatter}) = [(1-S)A(1-S)]^2 + [(1-S)(1-A)(1-S)]^2.$$

Let the probability that an atom survives n sweeps be $1/e$; then the momentum change for an atom at the point when it has probability $1/e$ not to be lost is

$$\begin{aligned}n \langle \Delta p_{\mathrm{SWAP}} \rangle &= \frac{\langle \Delta p_{\mathrm{SWAP}} \rangle}{-\ln\left(P(\text{no scatter})\right)} \\ &= \left(\frac{(1-x^Q)(x(2x^Q-1)-1)}{\ln\left(x^2 + 2x^{Q+2}(x^Q-1)\right)}\right) \times 2\hbar k. \end{aligned} \tag{A.2}$$

This function is plotted in figure A2(b) for $Q = 25$ and maximized with respect to sweep rate in figure 4(b).

The optimal sweep rate for transferring momentum in the model where scattering is unimportant is found by taking the derivative of (A.1) with respect to α and equating it to zero:

$$\alpha_{\mathrm{opt}} \approx \frac{\pi}{2} \frac{\Omega^4}{4\Delta^2} \frac{1}{\ln\left[2\left(1+Q\right)\right]}. \tag{A.3}$$

However, the optimal sweep rate for transferring momentum before atoms are lost to recoiled photons (A.2) could only be found numerically (figure A2(a)). The scaling at significant Q remains the same as in (A.3) – the optimal sweep rate can be increased as roughly Ω^4/Δ^2 (though Q also changes as Ω^2).

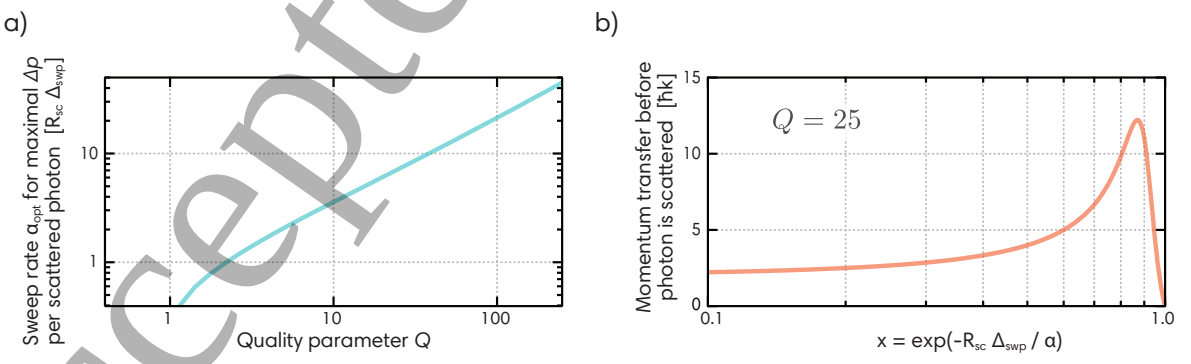

Figure A2. **(a)** The momentum transferred during a single simulated SWAP cooling sweep was found and maximized with respect to the sweep rate α. When the quality parameter Q is very small, the ideal strategy is to sweep very slowly in order to coherently scatter once. When Q is large, efficient adiabatic sweeps are possible. **(b)** The maximum momentum transferable before a photon scatters due to Raman cooling beams or optical pumping beams.

References

[1] Chu S, Bjorkholm J, Ashkin A and Cable A 1986 *Physical Review Letters* **57** 314

[2] Diedrich F, Bergquist J, Itano W M and Wineland D 1989 *Physical Review Letters* **62** 403

[3] Chan J, Alegre T M, Safavi-Naeini A H, Hill J T, Krause A, Gröblacher S, Aspelmeyer M and Painter O 2011 *Nature* **478** 89–92

[4] Stellmer S, Pasquiou B, Grimm R and Schreck F 2013 *Phys. Rev. Lett.* **110**(26) 263003

[5] Duarte P M, Hart R A, Hitchcock J M, Corcovilos T A, Yang T L, Reed A and Hulet R G 2011 *Phys. Rev. A* **84**(6) 061406

[6] Ido T, Isoya Y and Katori H 2000 *Phys. Rev. A* **61**(6) 061403

[7] Loftus T H, Ido T, Ludlow A D, Boyd M M and Ye J 2004 *Phys. Rev. Lett.* **93**(7) 073003

[8] Vogel K R, Dinneen T P, Gallagher A and Hall J L 1999 *IEEE Transactions on Instrumentation and Measurement* **48** 618–621

[9] Berglund A J, Hanssen J L and McClelland J J 2008 *Phys. Rev. Lett.* **100**(11) 113002

[10] Wallis H and Ertmer W 1989 *J. Opt. Soc. Am. B* **6** 2211–2219

[11] Katori H, Ido T, Isoya Y and Kuwata-Gonokami M 1999 *Phys. Rev. Lett.* **82**(6) 1116–1119

[12] Binnewies T, Wilpers G, Sterr U, Riehle F, Helmcke J, Mehlstäubler T E, Rasel E M and Ertmer W 2001 *Phys. Rev. Lett.* **87**(12) 123002

[13] Teufel J D, Donner T, Li D, Harlow J W, Allman M S, Cicak K, Sirois A J, Whittaker J D, Lehnert K W and Simmonds R W 2011 *Nature* **475** 359 EP –

[14] Chan J, Alegre T P M, Safavi-Naeini A H, Hill J T, Krause A, Gröblacher S, Aspelmeyer M and Painter O 2011 *Nature* **478** 89 EP –

[15] Hosseini M, Duan Y, Beck K M, Chen Y T and Vuletić V 2017 *Phys. Rev. Lett.* **118**(18) 183601

[16] Corder C, Arnold B and Metcalf H 2015 *Phys. Rev. Lett.* **114**(4) 043002

[17] Rochester S M, Szymański K, Raizen M, Pustelny S, Auzinsh M and Budker D 2016 *Phys. Rev. A* **94**(4) 043416

[18] Prehn A, Ibrügger M, Glöckner R, Rempe G and Zeppenfeld M 2016 *Phys. Rev. Lett.* **116**(6) 063005

[19] Dunning A, Gregory R, Bateman J, Himsworth M and Freegarde T 2015 *Phys. Rev. Lett.* **115**(7) 073004

[20] Shuman E S, Barry J F and DeMille D 2010 *Nature* **467** 820 – 823

[21] Hummon M T, Yeo M, Stuhl B K, Collopy A L, Xia Y and Ye J 2013 *Phys. Rev. Lett.* **110**(14) 143001

[22] Zhelyazkova V, Cournol A, Wall T E, Matsushima A, Hudson J J, Hinds E A, Tarbutt M R and Sauer B E 2014 *Phys. Rev. A* **89**(5) 053416

[23] Kozyryev I, Baum L, Matsuda K, Augenbraun B L, Anderegg L, Sedlack A P and Doyle J M 2017 *Phys. Rev. Lett.* **118**(17) 173201

[24] Kozyryev I, Baum L, Aldridge L, Yu P, Eyler E E and Doyle J M 2018 *Phys. Rev. Lett.* **120**(6) 063205

[25] Norcia M A, Cline J R K, Bartolotta J P, Holland M J and Thompson J K 2017 *New J. Phys.* **20** 023021

[26] Miao X, Wertz E, Cohen M G and Metcalf H 2007 *Phys. Rev. A* **75**(1) 011402

[27] Petersen N, Mhlbauer F, Bougas L, Sharma A, Budker D and Windpassinger P 2018 Sawtooth wave adiabatic passage slowing of dysprosium (*Preprint* arXiv:1809.06423)

[28] Muniz J A, Norcia M A, Cline J R K and Thompson J K 2018 A robust narrow-line magneto-optical trap using adiabatic transfer (*Preprint* arXiv:1806.00838)

[29] Snigirev S, Park A J, Heinz A, Bloch I and Blatt S 2019 Fast and dense magneto-optical traps for strontium (*Preprint* arXiv:1903.06435)

[30] Chab J, Lignier H, Szriftgiser P and Garreau J C 2007 *Optics Communications* **274** 254 – 259 ISSN 0030-4018

[31] Aspect A, Arimondo E, Kaiser R, Vansteenkiste N and Cohen-Tannoudji C 1988 *Phys. Rev. Lett.*

61(7) 826–829
[32] Davidson N, Lee H J, Kasevich M and Chu S 1994 *Phys. Rev. Lett.* **72**(20) 3158–3161
[33] Hu J, Urvoy A, Vendeiro Z, Crépel V, Chen W and Vuletić V 2017 *Science* **358** 1078–1080 ISSN 0036-8075 (*Preprint* https://science.sciencemag.org/content/358/6366/1078.full.pdf)
[34] Dalibard J and Cohen-Tannoudji C 1989 *J. Opt. Soc. Am. B* **6** 2023–2045
[35] Bateman J and Freegarde T 2007 *Phys. Rev. A* **76**(1) 013416